Transparent and Colored Solar Photovoltaics for Building Integrations

Zhenpeng Li, Tao Ma, Hongxing Yang, Lin Lu, Ruzhu Wang*

Z. Li, Dr. T. Ma, Prof. R. Wang
Engineering Research Centre of Solar Energy and Refrigeration of MOE, School of Mechanical Engineering
Shanghai Jiao Tong University
Shanghai 200240, China
E-mail: tao.ma@connect.polyu.hk

Prof. H. Yang, Prof. L. Lu
Renewable Energy Research Group, Department of Building Service Engineering
The Hong Kong Polytechnic University
Hong Kong, China

Keywords: solar energy, solar cells, building-integrated photovoltaics (BIPV), transparent PV, colored PV

Building-integrated photovoltaic (BIPV) stands as a promising solution to provide renewable electricity for achieving zero energy buildings, while still hindered from large-scale implementations due to the difficulty of traditional photovoltaic modules in meeting the standards and aesthetics of architectural materials. Emerging of new photovoltaic materials and devices could pave the way for the future, through offering diversity and tunability in colors and transparency along with comparable performance. This review has discussed the recent advances in BIPVs, starting from an overview of various photovoltaic technologies regarding their material characteristics, state of the art and the adaptability to the built environment. The transparent and colored photovoltaic technology are then respectively emphasized, concerning design principles, theoretical analysis, technical routes and corresponding demonstration studies. The various strategies including the materials and structures adopted to modifying the transparency and color in solar cells are extremely highlighted. Finally, the challenges and future perspectives are addressed, followed by an outlook of factors which are critical for large-scale implementations of BIPVs in the future.

1. Introduction

To address climate change and promote sustainable development, the energy transition is nowadays a key issue of the global economy and society, driving rapid development of renewable energy, energy conservation, emission reduction, electrification and smart management technologies. However, global energy consumption is still growing, with the building sector always accounting for more than a third (**Figure 1**a).[1] In order to achieve global climate objectives by 2050, the energy consumption in buildings thus has to be reduced, while meanwhile renewable energy, especially renewable electricity must become a major part of building energy source (**Figure 1**b).[2] With such an immense challenge, governments around the world are prompting critical requirements on energy-efficiency buildings, along with growing incentives to building energy-saving technologies.[3] Photovoltaics (PV), which directly capture sunlight and convert it into electricity, are considered as the most important building-adapted renewable energy technology, since they can be widely deployed on building facades and roofs worldwide to quietly provide clean electricity.

The last decade has seen tremendous growth in the PV market, mainly in the relatively large-scale power plants whose capacities are over megawatts. With a rapid decline in PV cost and the realization of grid parity,[4] more and more PV modules are being installed on buildings to help for energy saving and even as a means of investment. Most of these PV modules are additively adhered to existing buildings as separate parts (aka building-applied/attached photovoltaic, BAPV), which is easy to be implemented, but provides poor architectural aesthetics and poses great limitations on installation conditions. To cover all the available installation areas of building facades and roofs in a better way, the building-integrated photovoltaics (BIPV), which has dual functions of not only power-generating components, but also construction materials for building envelope and decoration, are considered a more desirable solution. The benefits of BIPVs are clear, attractive for a broad range of

stakeholders to pay attention, while the progress in practical applications is limited, except for some showcases at exhibitions or demonstration projects.[5] Factors that may hinder BIPV development in the past are complex, but the present-day conditions that will drive the growth of BIPV markets are maturing: on the supply side, PV companies are looking for exploiting niche markets to avoid brutal competition in traditional markets, while on the demand side, huge pressure on the building energy saving is calling for BIPVs especially in urban areas. Consequently, it is estimated that the BIPV market could grow by nearly 40% per year in the following decade (**Figure 1**c).[5]

No matter how strong these drivers of market growth are, the distance from a single power-generation component to a truly qualified building material is still long and tough, requiring the PV sector itself to address those technical obstacles on the road. The primary challenge is to make BIPV products comparable to traditional building materials in aesthetics, while maintaining a certain level of performance. Current PV products applied on buildings are generally based on crystalline silicon (c-Si) solar cells, as well as some inorganic thin-film technologies, which are dedicatedly designed for maximizing the ability to generate power. Since a good PV material generally has a bandgap lower than 1.85 eV, and thus a cut-off absorption wavelength beyond the range of visible light (VIS) spectrum, the PV module is always designed to absorbed as much VIS as possible to obtain high output current. Consequently, these solar PV panels are generally opaque, showing black or dark-blue color (**Figure 2**a), with the most aesthetic one among them just in a uniform black appearance, far from the requirements of diversified architectural design and styles. In this context, BIPVs are supposed to undergoing some modifications to selectively reflect specific visible light, thus producing colored outlooks (**Figure 2**b). Although the reflection will inevitably cause a reduction in power conversion efficiency (PCE) when compared to black ones, such opaque PV products with customizable colors are essential to cover the huge installation potentials on

worldwide building roofs and facades. Besides color, transparency is another critical factor for BIPVs, to tap the remaining substantial building areas which allow for natural lighting, such as windows, skylights and glass curtain walls. Semi-transparent or transparent PV (STPV or TPV, uniformly referred to as TPV in this paper), which considers both light transmission and absorption, are getting more and more concerned to address this issue. Provided there exists uniform spectral transmittance in VIS, solar cells will be semi-transparent and neutral-colored, similar to common building glass (**Figure 2**c). Otherwise, when the spectral transmittance varies in VIS, TPV products could also be colored, favorable for applications in some architectural decorations (**Figure 2**d).

Thanks to the advances in emerging PV materials, as well as innovative designs in PV devices and modules, the customized modification in color and transparency of solar PVs attracts more and more attentions, enabling a wide development prospect of aesthetic BIPV products in the future. Herein, a comprehensive review is presented on the recent advances in the PV research field intending for BIPV applications, mainly the transparent PV technology and colored PV technology, with respect to theoretical analysis and a thorough investigation of different technical routes. An overview of the mainstream solar PV technologies is first presented, involving the material characteristics and development status, to briefly analyze their potential advantages and disadvantages in the development of BIPVs. Subsequently, the TPV technology based upon spatial segmentation, wavelength-selective absorption, and the structure of luminescent solar concentrators is respectively discussed, to illustrate their potential in theory and representative demonstrations. We then provide a theoretical guide for modification in PV color, and go on to discuss diverse strategies that have been employed for c-Si and emerging thin-film solar cells, in which their colors are independent on solar cell materials. Finally, some crucial challenges/opportunities are put forwarded to promote the

development of aesthetic BIPVs toward new horizons, followed by some perspectives on large-scale implementation of BIPVs in the future.

2. Overview of Solar Photovoltaic Technologies

Along with the improvement in efficiency and decrease in cost, c-Si PV technology is still dominating the market of ground power stations and distributed applications. Thin-film PVs based on CdTe, CIGS and amorphous Si (a-Si), once believed to be competitive against c-Si in niche markets like BIPVs, have not achieved expected success in the past decade. In this context, identifying the strength and weakness of different PV technologies in the application of building environment is of vital importance, since substantial semiconductor materials have been discovered to develop a variety of solar cells in the last half-century.

The different properties of semiconductor materials and their bandgaps are usually employed to distinguish PV technologies. **Figure 3**a shows the efficiency limit of single-junction solar cells as a function of bandgap under standard AM1.5 solar spectrum, derived from the detailed-balance theory developed by Shockley and Queisser (S-Q limit).[6] The record efficiency of present-day 'champion' solar cells is also plotted in the figure, which could be recognized as an indicator of the progress of these PV technologies. However, as many other properties also play critical roles, the method based on only bandgap is deficient to evaluate the potential in the PCE and the BIPV applications. In this context, here we classify widely studied PV technologies into four groups with respect to large-scale BIPV applications, according to material characteristics and the development stage.

Not Recommended

Solar cells made by III-V compound semiconductor materials are not recommended for BIPV despite their remarkable PCE values. Due to the high production cost, GaAs is restricted in

some special markets which demand high efficiency while the cost is rarely a consideration, such as space technologies.[7] Emerging technologies enabling low-cost and large-scale production of GaAs might make a change, but the toxicity of As and the scarcity of Ga may still hinder it from wide applications in civil uses. A similar situation exists for InP and GaInP, as well as multijunction solar cells stacked by those III-V group materials. Consequently, in the foreseeable future, it is hard to witness large scale implementations of these technologies in the field of BIPVs.

Sustainable and Commercialized

Crystalline-Si PV technology including single-crystalline Si and multicrystalline Si (mc-Si) holds the most share of PV market due to the high performance and long-term reliability. Comparing with GaAs, lower production cost and readily accessible Si elements are tremendous advantages. Especially, the mature industrialization and commercialization process is continually moving the c-Si PV forward, keeping its first-mover advantage in various markets involving the building market. However, a relatively thick wafer of 100-200 μm because of the relatively lower absorption coefficient, makes c-Si the only non-thin-film solar cell, and have poor performance under the conditions of low light and large incident angle. Therefore, thin-film Si solar cells that claim their advantages in flexible PV products is developed, such as a-Si and microcrystalline Si (μc-Si). Due to their intrinsic material limitations, those solar cells show relatively low efficiency and little progress has been witnessed in recent years.[8] Both c-Si and thin-film Si PVs have been applied on buildings.

Commercialized but Restricted

The CdTe and $Cu(In,Ga)(Se,S)_2$ (CIGS) solar cells are two commercialized thin-film technologies with PCE records above 22%, and the module efficiency approaches 19%.[9] In this context, they used to be ones with expectations for substituting c-Si at least in some niche

markets. In 2019, CdTe solar modules took over 90% of the thin-film PV market, while the majority was installed in ground power stations. Public concern about CdTe focuses on the toxicity of element Cd and scarcity of element Te, leading to requirements for rigorous encapsulation and effective recycling systems. CIGS PVs also face similar problems. To address fierce competition with c-Si PV technology, further efficiency improvement, cost reduction, along with exploiting new markets like the BIPV, are critical for CdTe and CIGS solar PV technologies.

The dye-sensitized solar cell (DSSC) is not a traditional PV technology based on solid semiconductor materials, whereas molecular dyes, usually organometallic complex or purely organic, serve for absorbing light and exciting electrons.[10] Because of a voltage loss during electron transfer and large current losses due to a narrow absorption band, the performance of DSSC is intrinsically uncompetitive. However, the unique mechanism enables DSSC the first class of PV technologies with the availability of intrinsic various colors and a simple fabrication process. In other words, DSSC looks dedicated to non-station applications such as buildings and mobile devices. Commercial DSSC products are already available, while the market share seems negligible due to the disadvantages like low efficiency, poor outdoor stability and the use of liquid electrolytes.[11] In view of the development history of solar cells, DSSC is mainly credited with its inspiring research into organic and perovskite solar cells, but the DSSC itself may not be wildly applied.

Emerging

$Cu(Zn,Sn)(S,Se)_2$ (CZTS) is regarded as the sustainable succedaneum of CIGS by replacing In and Ga with less expensive and more earth-abundant elements. Nevertheless, the large intrinsic voltage loss due to material defects is the major obstacle, making the actual efficiency far below the value predicted by the S-Q theory.[12] In quantum dot (QD) solar cells,

the absorbing layer is made by nanoscale semiconductors, which could be synthesized by solution processing and possess tunable bandgap, thus offering probability in making more flexible PV products for distributed applications. Metal halide materials dominate QD solar cells in recent years, and bring great efficiency improvement.[13, 14]

Solar cells based on ABX_3 metal halide perovskites have achieved remarkable progress in the past decade, mainly due to their excellent material properties such as high absorption coefficient, great defect tolerance, and long diffusion length.[15] It is recognized that perovskite solar cells have combined the advantages of thin-film PV technologies with the good performance and sustainability of c-Si, enabling them the most promising PV technology to be implemented in any scenarios on a large scale. Challenges primarily relate to the scalability, toxicity of Pb and long-term stability, whereas recent research has shown its great progress.[16, 17]

Benefit from the development of material design, inspiring progress has also been witnessed in the PCE of organic solar cells in recent two years.[18] Although using organic materials leads to inevitable energy losses in charge separation and relatively high rate of non-radiative recombination,[19] it offers a wide choice of materials and low-cost fabrication process, thus bringing the widest availability in flexibility, color and transparency. In this context, the organic solar cell is supposed to substitute the role played by DSSC, on condition that issues of scalability and long-term stability could be well addressed.

Overall, solar PV technologies based on c-Si, a-Si, CdTe, CIGS are nowadays available in the BIPV market, having their own merits and demerits respectively, while the emerging perovskite and organic solar cells show great potentials in providing a better solution for BIPV applications. As demonstrated in **Figure 3**b, the high-efficiency solar cells based on

these PV technologies similarly show high EQE in the wavelength range coving VIS light, meaning their strong VIS absorption and thus black appearance. To enable transparent or colored appearance, efforts should be devoted to modifying the optical characteristics, simultaneously maintaining as high EQE as possible. Many practices on either commercialized or emerging solar PV technologies have been demonstrated in the literature, using different technical routes regarding different material characteristics. Those issues will be covered in great details in the following sections.

3. Transparent Photovoltaic Technologies

To evaluate the performance of TPVs, an index, i.e. average visible transmittance (AVT), was introduced, which is calculated as average spectral transmittance of light in the VIS wavelength range weighted by the photopic response of human eyes:

$$AVT = \frac{\int_{\lambda_1}^{\lambda_2} T(\lambda)V(\lambda)I(\lambda)d\lambda}{\int_{\lambda_1}^{\lambda_2} V(\lambda)I(\lambda)d\lambda} \quad (1)$$

where λ is the wavelength, $T(\lambda)$ is the spectral transmittivity of the device evaluated, $V(\lambda)$ is the luminous efficiency function, $I(\lambda)$ is the illuminant function, and (λ_1, λ_2) is the integral range covering the wavelength of VIS light. Considering that there appears slight divergence in the calculation of AVT, and no uniform standard for TPVs has been established yet, the regulation in the building glass industry is suggested as a major reference.[20] In this standard, $V(\lambda)$ should be the photopic luminosity function established by International Commission on Illumination (CIE), $I(\lambda)$ is the CIE standard illuminant D65 that defines the relative spectral power distribution of average daylight,[21] λ_1 is 380 nm and λ_2 is 780 nm.

In the research field of solar PVs, the AM1.5 solar spectral irradiance is wildly used for characterizing PV performance. Considering that in practical deployment, a TPV device will

be illuminated by only one type of incident solar spectrum, it is recommended to also adopt AM1.5 as the light source for characterizing the AVT. This is a practice in many previous studies and is suggested by Traverse et al.[22]. Besides, in the literature both the AM1.5 data measured in energy flux (W m^{-2} nm^{-1}) and photon flux (m^{-2} nm^{-1} s^{-1}) have been adopted. Considering that D65 is a measure of power distribution of the illuminant, we recommend using energy flux for AVT calculation, holding different views with Yang et al.[23] Although $V(\lambda)$ is nonzero in the wavelength range of 380-780 nm, using the range of (400 nm, 700 nm) will not make difference since the $V(\lambda)$ outside this range is negligible (smaller than 0.004). Furthermore, as claimed by Lunt et al.[24] in their theoretical analysis, the range of (435 nm, 670 nm) is sufficient to cover over 99% of VIS light, which can be a guide principle for designing TPVs, indicating that high absorptivity while small transmissivity in (380 nm, 435 nm) and (670 nm, 780 nm) will not significantly decrease the AVT.

In this paper, the TPVs only indicates those neutral-colored ones as shown in **Figure 2**c, which should provide a clear and non-discoloring view through the BIPV products and could be evaluated by the figures of merit as color rendering index (CRI) and CIELAB color coordinates (a^*, b^*).[23] In this context, to improve AVT while minimizing impacts on PCE is the focus in this research field. With the development of various solar cell materials described above, different strategies are employed to modify the AVT with respect to different material characteristics, involving spatial segmentation, wavelength-selective absorption, and luminescent solar concentrators.

3.1 Spatial Segmentation

As illustrated in **Figure 4**a, spatial segmentation is a common strategy through removing part of absorption materials in solar cells, which are encapsulated by both transparent covers and backsheets. Thus, the solar radiation illuminating on the transmission region can be fully

permeated for day lighting. In ideal cases, the void fraction (the ratio of transmission region and total PV area) should be equal to the spectral transmittance of solar cells when the wavelength is smaller than the cut-off value, and also the AVT, since VIS is usually within this wavelength range for most PV materials (**Figure 4**b). Consequently, higher AVT can be simply realized by enlarging the space between absorption regions, at the cost of a linear decrease in short-circuit current (J_{sc}) due to reduced photoactive materials (**Figure 4**c). The open-circuit voltage (V_{oc}) and fill factor (*FF*) are ideally invariable, while in practice they might be inevitably reduced due to some damage from material segmentation,[25] especially on the condition of a high AVT value.

In this context, spatially segmented TPVs may be only suitable for conditions requiring for relatively low AVT, whereas their superiority is the applicability to all types of PV materials.[22] Early practices appear in c-Si solar cells,[26, 27] but since the prefabricated silicon wafer is relatively thick, segmental removement of Si materials is generally not economical through either mechanical cutting or laser cutting. The alternative strategy is directly manufacturing thin and narrow c-Si wafers, which are then arranged together at a certain distance as shown in **Figure 5**a.[28, 29] There exists no such trouble for thin-film PV technologies such as CIGS, CdTe and a-Si PVs due to their very thin semiconductor films (~1-2μm), made by using sputtering or evaporation in a large area. Therefore, the laser scribing has already been employed in the fabrication process to split cells and make electrical connections,[30] as demonstrated in P1-3 in **Figure 5**c. Only if another laser scribing process P4 is introduced, an opaque PV module can be transformed into a semi-transparent one (**Figure 5**b).[25, 31] This great compatibility of manufacture process enables TPVs based on CIGS, CdTe and a-Si be already commercialized, and account for the majority of available TPV products.

Nevertheless, the inhomogeneous appearance of spatially segmented TPVs due to visible absorbing materials may hinder their acceptability to markets. A recent study claimed that neutral-colored semitransparent c-Si solar cells could be achieved through making microscale holes within microscale distance on the c-Si wafer.[32] Due to the ultrashort distance between the hole-shaped transmission regions along with any directions, intervenient absorption materials become visually invisible, resulting in a favorable appearance and competitive performance against those thin-film TPV products (**Figure 5**e). Photolithography process and deep reactive ion etching (DRIE) process (**Figure 5**d) were employed to fabricate the microhole arrays on c-Si wafers, while the issues such as cost and compatibility with existing industrial production line could be the main obstacles.

Different from above inorganic solar cells, the easy fabrication process of DSSC, organic and perovskite thin films enable controlling of material growth morphology to directly build spatially segmented TPVs, being more material-saving and economical against those post-processing methods. The practice mainly focuses on perovskite solar cells,[33] including self-assembly of a perovskite grid structure (**Figure 5**f),[34] controlling evaporation rate to form microstructured perovskite islands (**Figure 5**g),[35, 36] and using SiO_2 honeycomb scaffold template to deposit patterned perovskite films (**Figure 5**h).[37, 38] Since these microscale structures of perovskite films are undetectable for human eyes, neutral-colored and glass-look perovskite TPVs can thus be easily obtained as long as the devices have uniform transmittance in the wavelength range of VIS light. The best result of a PCE at 10.3% has been obtained, along with an AVT of 38%,[38] showing a brilliant prospect of this technology.

3.2 Wavelength-selective Absorption

From the theoretical-limit point of view, a TPV should only transmit VIS light to ensure high PCE, while the UV light (<435 nm) and NIR light (>670 nm), which cannot be detected by

human eyes unless strong enough, should still be absorbed by solar cells to generate electricity. In this context, solar cells with the characteristic of wavelength-selective absorption and strong VIS light transmission, which are called as wavelength-selective TPVs (**Figure 6**a), are emerging in recent years. As displayed in **Figure 6**b, varying the AVT of an ideal wavelength-selective TPV affects EQE only in the wavelength range of VIS light. Even though for an AVT of 100%, the remaining 65% of solar energy can still be a significant source for power generation.

By applying these ideal EQE curves displayed in **Figure 6**b to the S-Q limit model, the efficiency limit of the wavelength-selective TPV (single junction) can be calculated based on the work of Lunt et al.[24]. As presented in **Figure 6**c, an increase in AVT will inevitably reduce PCE of solar cells for all bandgaps, whereas higher bandgap suffers more loss in PCE, due to that VIS light contributes more in high-bandgap solar cells. Consequently, the optimal bandgap is also reduced with AVT increasing, showing a redshift from 1.34 eV (opaque) to 1.12 eV (AVT=100%), with the corresponding maximum efficiency decreasing from 33.7% to 20.6%. Taking a bandgap of 1.12 eV (Si) for example, a wavelength-selective TPV shows evident advantages in the PCE limit against a spatially segmented one, particularly when a high AVT is essential (**Figure 6**d), proving a roadmap for developing a real sense of TPV products.

The wavelength-selective absorption means critical requirements on materials, whereas those common solid semiconductors cannot meet, since that the continuous energy bands of semiconductors lead to continuous photon absorption once the photon energy exceeds the bandgap (E_g). Thus, NIR-selective harvesting is intrinsically prohibited in semiconductors. Only when the bandgap is above 2.85 eV (435 nm), a semiconductor could absorb only UV light and thus transmit all light above 435 nm including VIS light. But for a solar cell based

on such high-bandgap materials, its S-Q efficiency limit is only 6.4%, imposing great restrictions on performance.

Practices in literature start from using some metal oxide semiconductors, such as NiO and ZnO, while only fractional photocurrents can be detected, resulting in the PCE pretty low.[39, 40] Emerging of ABX_3 perovskite materials in recent years provides new solutions due to their good bandgap tunability and great success in developing high-PCE solar cells. By substituting the halide from a bigger one to a smaller one (I^->Br^->Cl^-), the absorption onset of perovskites will gradually blue-shift, making solar cells finally be UV-selective and thus visibly transparent. The first demonstration of perovskite-based TPV devices was reported by Liu et al.[41] in 2018, with either $MAPbCl_3$ (E_g=3.04 eV) or $MAPbCl_{2.4}Br_{0.6}$ (E_g=2.83 eV) as photoactive materials. $MAPbCl_{2.4}Br_{0.6}$-based devices performed better, with the best one at a PCE of 0.52%, along with an AVT of 73% and a CRI of 93.8 (**Figure 7**a and **Figure 7**b). Since this prototype only has an EQE of 20-30% and a FF of 45%, a future PCE value approaching 4% is in prospect when an EQE above 90% can be realized.[41]

As for the NIR-selective absorption, solutions are given by solar cells based on polymer or small-molecule organic materials,[42] which have different mechanisms in optical absorption with those solid semiconductors. Due to the nature of relatively discrete molecular orbitals, absorption of organic materials is not continuous, but has a peak as well as a start point and end point. This mechanism is originally a defect as it limits the light absorption, however now turns to be irreplaceable for developing high-performance TPVs.[43] The report on a NIR-selective organic TPV firstly came out in 2011,when Lunt et al.[44] pioneered the field by using a planar heterojunction structure, consisting of C_{60} as the acceptor and chloroaluminum phthalocyanine (ClAlPc) as the donor, whose absorption peak is positioned at 740 nm. Although only a PCE of 1.7% was achieved with an AVT of 56%, a new door to high-

performance TPVs was opened since then. Afterward, many low-bandgap organic materials including donors and acceptors are developed for NIR-selective TPVs, which can refer to Ref.[43],[45], while here several representative devices are focused to show the progress.

Figure 7c and **Figure 7**d present an impressive work reported by Chen et al.[46]. They utilized the PBDTT-DPP (donor) and PCBM (acceptor) to form a bulk heterojunction blend as the photoactive layer, which was sandwiched between two transparent electrodes (top: Ag NW-based composite, bottom: ITO). Since the PBDTT-DPP: PCBM layer achieved an average transmission of 68% over the range of 400-650 nm, a device with a high AVT of 64.4% and an improved PCE of 4.01% was realized. This work represented a typical design in that stage, i.e. a BHJ film consisting of a low-bandgap polymer donor and a fullerene acceptor, sandwiched by transparent electrodes.[47-53] Despite many efforts have been made to the novel material design and bandgap engineering, the bandgap of those polymers was still not low enough to harvest more NIR photons, especially for the fullerene acceptor materials, whose energy levels can scarcely be tuned.

Recently the emerging of non-fullerene small molecules as acceptors has paved the way to further improving the performance of organic solar cells,[54, 55] stimulating organic TPVs enabled by both NIR-response donors and acceptors.[56-59] Generally, TPV devices developed through this strategy since 2017 possess the PCE of 7%-10%, along with the AVT of 30-50%, showing significant improvement in performance. For instance, Liu et al.[60] recently demonstrated a remarkable device with a blend mixing a narrow bandgap acceptor as FOIC and a donor as PTB7-Th, achieving an absorption band peaking at 820 nm (**Figure 7**e).[58] Although a standard solar cell only showed a PCE of 5.75%, by adding a 1D nanophotonic structure consisting of low and high refractive index dielectric layers, the EQE in NIR was greatly enhanced to increase the PCE to 8.32%, on the condition of keeping an AVT over

50% (**Figure 7**f). This example reveals that for TPV design the light management is as critical as absorbing materials. Actually, most organic materials still uniformly absorb in the wavelength of VIS, leading to a recognizable color. This issue can also be dealt with adding dielectric layers to modify the spectral transmittance, thus to enable a real sense of neutral-colored TPV.[61]

Based on above-mentioned either UV-selective TPVs or NIR-selective TPVs, it is natural to develop a tandem structure for both the UV and NIR light harvesting and further performance improvement, which was demonstrated by Zuo et al.[62] (**Figure 7**g and **Figure 7**h). They applied $FAPbBr_{2.43}Cl_{0.57}$ (E_g=2.26 eV) to make the top subcell that mainly harvests UV light, and PTB7-Th: 6TIV-4F the bottom subcell that mainly harvests NIR light. This strategy successfully provided a much improved PCE of 10.7%, along with an AVT of 52.91%, considered as the most outstanding performance in recent years.

3.3 Luminescent Solar Concentrators

Luminescent solar concentrator (LSC) offers another way for realizing transparent PV glass by separating the light harvest components from solar cells. A typical LSC consists of a glass or polymer waveguide and solar cells attached at its edges. Incident light is firstly harvested by chromophores embodied in the waveguide, and then re-emitted at longer wavelength to be guided through total internal reflection until reaching edge-mounted solar cells (**Figure 8**a).[63] In this context, areas of solar cells are reduced in LSC systems, and a clear view is easily realized since there are no electrodes exposed. Moreover, the color and transparency of LSCs can be adjusted to a great extent by regulating the type and density of chromophores.

To enable neutral color for LSCs, chromophores embodied in waveguides must satisfy specific optical properties in light absorption and re-mission. As illustrated in **Figure 8**b, there

are basically three cases. In the first case, the absorption spectra of chromophores locates in the wavelength range of UV light, while photoluminescence (PL) spectra in the wavelength range of NIR light, indicating a massive Stokes-shift. This idea was demonstrated by Luo et al.[64], using Yb^{3+}-doped perovskite ($CsPbCl_3$) nanocrystals as the chromophore, which has a absorption cutoff in 400 nm and can re-emit from 900 nm, providing a wide VIS window (**Figure 8**c). Such a massive downshift originates from the quantum-cutting effect, by which one absorbed UV photon is down-shifted to two emitted NIR photons.[64] Besides, a photoluminescence quantum yield approaching 200% is achievable by this mechanism, making chromophores with the quantum-cutting effect be more superior candidate for UV-harvesting LSCs. By the massive downshift, reabsorption losses are avoided, but the small coverage of absorption spectra greatly limits its performance. Except for lanthanide complexes, metal halide clusters could also realize such a large shift.[65] Another strategy is to absorb NIR light and emit deeper-NIR photons. To avoid the light emitted by one chromophore being reabsorbed by another chromophore, the overlap area between absorption spectra and PL spectra must be restrained. Organic salt derivatives could help implement this mechanism, which was demonstrated by Zhao et al.[66] in 2014, providing a very high AVT of 86% and indistinguishable appearance against glass (**Figure 8**d). By adopting another organic molecule CO_i8DFIC recently, a PCE over 1.2% is achieved.[67] Nevertheless, those materials still show obvious overlaps between absorption spectra and PL spectra (**Figure 8**d), could hindering the performance of large-scale devices to a great extent.

Similar with wavelength-selective TPVs, developing NIR-emitting chromophores which absorb both UV and NIR light is more attractive, but has few signs of progress in past years except for a report on a device using Si naphthalocyanine (SiNc) as chromophores.[68] Recently Yang et al.[69] reported a new strategy, which introduces a dual-band selective-harvesting LSC, composed of two distinct waveguides. UV-selective phosphorescent

hexanuclear nanoclusters ($Cs_2Mo_6I_8(CF_3CF_2COO)_6$ NC) is coated on the top waveguide, and the bottom one is based on fluorescent organic small molecules (COi8DFIC/BODIPY) to selectively harvest NIR photons. By such a dual-band structure, a PCE over 3% is achieved in an active area around 25 cm^2, along with an AVT over 75% and a CRI of 90%, setting an outstanding example for developing transparent LSCs with high-performance.

Actually, wavelength-selective absorption, which means only a small fraction of the solar spectrum can be harvested, is not an essential condition for developing neutral-colored LSCs. If the chromophore can absorb in a large wavelength range coving VIS, a colorless LSC under sunlight is also achievable provided that absorption spectra in VIS are relatively uniform and the quantity of chromophores is modest.[70] In this case, some colloidal nanocrystals of narrow-gap semiconductors such as CuInSeS, rather than lanthanide complexes and organic dyes, are preferable candidates.[70, 71] As shown in **Figure 8**e, a LSC showing faint brown color was demonstrated by Meinardi et al,[72] which is based on ZnS-coated $CuInSe_xS_{2-x}$ quantum dots with large absorption coverage. With a CRI of 91, this LSC performed no significant distortion in color perception, and can reduce the sunlight penetrating rooms.

It is recognized that with the renaissance LSCs in recent years, great progress in chromophores has been achieved, making re-absorption no longer a main obstacle to wildly implementing LSCs. While it should be kept in mind that some reported "highly efficient" devices are based on a small device size, and the concentration factor of these LSCs remains a critical issue.[73] As presently LSCs are expected to be applied in solar glazing systems, optimizing the performance for large-area devices is critical for future development. In this context, the optical losses in the waveguide materials must be suppressed, demanding for more attention and efforts.[70]

4. Colored Photovoltaic Technologies

Except for those surfaces like windows, skylights, glass curtain walls which require transparency, most surfaces on buildings such as roofs and facades are, otherwise, opaque and highly required in the frontal appearance. To enable a sound integration with buildings, PV modules are thus required to be visually comparable with ordinary building materials like ceramics, stones, metals, concretes, or woods, varying greatly in colors and textures. Since high-performance PV modules are intrinsically black and dark (see **Figure 2**a), a significant challenge is posed to modify appearances of PV modules without obvious negative impact on electrical performance, with color being the main concern.

4.1 Design Principles and Methods

As illustrated in **Figure 9**a, the color of an object is determined by three factors, i.e. light source, spectral reflectance and the response of human eyes.[74] In color science, the D65 defined by CIE is generally used to represent daylight illumination, while similar with the calculation of AVT, it is recommended to uniformly adopt the AM1.5 spectral solar irradiance as the light source for charactering both PV performance and aesthetic quality. Besides, the $\overline{x}(\lambda)$, $\overline{y}(\lambda)$, $\overline{z}(\lambda)$ color matching functions are defined by the CIE to represent an average human's chromatic response.[75] Thus, the standard color of an object is only determined by its spectral reflectivity *R(λ)*, and can be represented by CIE 1931 XYZ tri-stimulus values, with X, Y, and Z respectively calculated by:[76]

$$X \text{ or } Y \text{ or } Z = \frac{\int_{\lambda_1}^{\lambda_2} R(\lambda) I(\lambda) \cdot \overline{x}(\lambda) \text{ or } \overline{y}(\lambda) \text{ or } \overline{z}(\lambda) d\lambda}{\int_{\lambda_1}^{\lambda_2} I(\lambda) \overline{y}(\lambda) d\lambda} \quad (2)$$

where (λ_1, λ_2) is also the wavelength range of VIS. Since $\overline{y}(\lambda)$ equals the photopic luminosity function *V(λ)*, *Y* actually represents the relative luminosity or the average visible reflectance (AVR), which is in the range of (0,1), with *Y*=0 corresponding to complete absorption (black)

and Y=1 complete reflection (white).[77] The XYZ values can further be transformed into the CIE 1931 xyY color space by:

$$x \text{ or } y = \frac{X \text{ or } Y}{X + Y + Z} \tag{3}$$

Once x and y decided, the chromaticity is uniquely located in the CIE 1931 xyY chromaticity diagram as shown in **Figure 9**a. With both relative luminosity (Y) and chromaticity (x, y), a color is therefore precisely defined. In this context, if the spectral reflectance of an opaque object is measured, we can immediately decide its standard color. Conversely, if an opaque PV module is expected to be modified to a specific color, its spectral reflectance curve should be first determined. But due to multiple reflectance curves may lead to one color, it is essential to involve another consideration here, that is, the influence of reflectance curves on the PCE. In theory, there exists a reflectance curve that can generate the desired color and meanwhile causes a minimum loss in photocurrent, which is the basic design criterion for the color modification of solar cells.

Accordingly, Halme and Mäkinen recently educed theoretical efficiency limits of ideal colored opaque (T=0) PVs, revealing that introducing color to an ideal black solar cell only produces a relative power loss of less than 14% when Y=0.25, meaning the S-Q efficiency limit is still over 29%.[77] As presented in **Figure 9**b, increasing the relative luminosity Y to make brighter colors will decrease the performance absolutely, while at a constant Y, the yellow-green color offers the best performance. More specifically, for various colors in the Macbeth ColorChecker chart, the corresponding efficiency limit of each one is presented in **Figure 9**c, which is between 28.9% and 32.9%. Even a complete white color still promises a PCE limit of 24.1%. Although the ideal reflectance spectra in literature can be only approached but never achieved, it is confirmed that the loss introduced after adding color to

solar cells could be acceptable, as long as some measures are taken to optimize the reflectance spectra whenever possible.[76-78] It should be noted that these theories also work for designing an ideal semitransparent solar cell with a specific color, in which the reflectance should be 0 and the spectral transmittance $T(\lambda)$ determines its color on the transmitted side.

In practice, the color change is mainly achieved through modifying the optical properties of different layers in a solar cell or just adding a new layer, to change the reflection characteristics. Generally, materials above the photoactive layer are required to be as transparent as possible, while the underlying layers should be reflective if the solar cell is opaque, or semitransparent if the solar cell is also semitransparent. In this context, if the photoactive material presents an inherent color, the whole device will thus present the same color. This is common in DSSC and organic solar cells, thanks to their diverse photoactive materials with different optical characteristics, but at the price that the PCE is relatively small due to limited light absorption ability (see **Figure 9**d and ref.[79-82]). Besides, perovskite offers a great advantage compared to other semiconductor materials, as the possibility to tune their bandgaps in a wide range. By adjusting A, B, and X sites of the ABX_3 perovskite materials, optical absorption edges are easily tunable within the 350-1200 nm, presenting different colors due to the incomplete absorption of VIS (**Figure 9**d).[15]

Although the bandgap tuning is practicable for some types of solar cells, it poses great limitations on absorbing materials and also the EQE of solar cells (**Figure 9**d). With above theoretical guidance, a common practice for all types of solar cells is thus to change only the reflectance in the selective wavelength range belonging to VIS light. This can be practically realized by modifying the optical properties of the glass cover, encapsulant, or absorbing layer surface, collectively referred to optical engineering in this paper (**Figure 9**e). As presented in

Figure 2b and **Figure 9**e, the optical engineering has already been practiced on c-Si PV modules to achieve various colors, setting a good example for other types of PV technologies.

4.2 Practices on c-Si PV Modules

As illustrated in **Figure 10**a, a c-Si PV module is generally with a structure of glass cover-encapsulant-solar cells-encapsulant-backsheet. One of the most popular techniques is to add a coating on the glass cover. Painting technologies developed in the glass industry have been firstly introduced, including silk-screen printing and digital ceramic printing.[83, 84] Since these paints will absorb and reflect lights, the performance of PV modules is inevitably affected, and the decreasing rate mainly depends on the printing degree and the color (type of paints). The significant advantage of such technology is easy to adopt as there is no need for altering the current PV fabrication process, while in-depth study is required to examine its performance and long-term durability in outdoor environment.

The deposition of a dielectric filter on the internal surface of glass can also allow customized regulating spectral reflectance in a real sense.[85] This filter, also named spectrally selective photonic crystal reflector or distributed Bragg reflector, is generally composed of multilayer films made of alternating high-index and low-index dielectric materials. By carefully designing the layers (material, thickness and number), a specific range of wavelength can be reflected to achieve the desired color (**Figure 10**b).[86] Besides, an etching treatment can be further applied on the external surface to produce diffuse reflection and avoid glare effects.[87] In this context, a nearly perfect colored glass cover can be produced, which can faultlessly hide the below solar cells and withstand degradation over time. Since most of the light can still be transmitted and harvested by the underlying solar cells, the performance in practice could achieve 80% of a normal one.[86] For a white PV panel fabricated at CSEM, its efficiency loss was reported as around 40%, with a PCE of 11.4% when the PCE of a standard

PV module is 19.1%.[88] This technique was successfully commercialized by a company SwissINSO in Switzerland, showing good demonstration effects in some BIPV projects.[84, 89]

One defect of the painting or coating on cover glass is that only a single color can be easily realized, and a high-resolution pattern is thus challenging to be painted on. Adding an interlayer is suggested, standing as an independent part between the glass cover and solar cells. By printing a pattern or graph on a transparent film, a customizable appearance, such as a pattern of bricks and timber, can be easily realized for PV modules (**Figure 10**c).[90] Since the printing inks are critical for PV performance, which should be transparent at least for the NIR light and also semitransparent for most VIS light, efforts are required to further investigate the long-term durability of such inks. No matter the specific methods used, this idea, which combines vivid prints and PV modules, could perfectly exhibit in some occasions as a integration of art and renewable energy.[91]

Another color modification technology of c-Si solar cells addresses on the anti-reflection coating (ARC), which is made by dielectric films that sputtered on the surface of c-Si solar cells to reduce light reflection (**Figure 10**d),[92] usually a SiN_x layer. To maximize the photocurrent, an ARC is generally optimized to make the spectral reflectance in 600-700 nm close to 0, resulting in a relatively high reflectance in the wavelength corresponding to blue light, thus an inherent color of either black or dark-blue of standard c-Si solar cells. By varying the thickness of ARC layers, the spectral reflectance curve can be easily regulated with different peaks in the VIS (see **Figure 10**d). In literature, Tobias et al.[93] and Zeng et al.[94] have respectively demonstrated c-Si solar cells with vivid colors involving blue, red, yellow and green, using different ARC materials. Test results show these colored solar cells achieved PCE over 16%.[94] Moreover, the double-layer or even triple-layer ARC system can be further explored if more colors need be accurately achieved.[95, 96] The greatest advantage

of the ARC modification is an acceptable loss, which could be less than 10% for many colors, as reported in literature.[94, 96] Thanks to simple integration with existing production process, this technique seems to be an ideal solution to produce colored c-Si PV products, but is only applicable to c-Si.

Some other practices are also proposed for colored c-Si solar cells, such as applying metal (Ag) nanoparticles on the surface of c-Si solar cells to produce color by plasmonic scattering,[97] and using dielectric (Si) nano scatters to produce bright scattering colors due to the excitation of Mie resonances.[98] The details of these plasmonic resonators are not covered here as they have no significant advantages over the technologies discussed above.

4.3 Practices on Thin-film Solar Cells

When talking about colored thin-film solar cells, a semitransparent one normally comes into mind firstly, since it is relatively easy to be achieved by just decreasing the thickness of the absorbing layer and the metal contact, or substituting the metal contact with other transparent materials. However, thin-film solar cells made by this method generally present only brownish red, especially for those inorganic materials like a-Si, CIGS, CdTe and also the perovskite.[31] Such an appearance is not favorable in most cases. As mentioned above, DSSC and organic solar cells could provide rich colors by varying absorbing materials, while the PCE is limited. Herein, some representative color modification methods are addressed that have been respectively practiced on opaque and semitransparent thin-film solar cells, with their color independent on the absorbing materials.

4.3.1 Opaque Devices

The aforementioned coloring technologies being applied to packaging materials of c-Si PV modules are also practicable for thin-film PV technologies, such as the dielectric-film coating

on the glass cover. For instance, a Bragg reflector consisting of dielectric films can be deposited between the front glass and the transparent conducting oxide (TCO) layer, which is an additional but compatible production process for commercialized thin-film solar cells (**Figure 11**b).[31] By combining this technology with the segment laser scribing as mentioned in Section 3.1, semitransparent modules with different colors are also available.[99, 100] Besides, this wavelength-selective reflector can also be integrated into the electron transport layer (ETL) in some types of solar cells, since the TiO_2 widely used in the ETL is also a dielectric material with high reflective index. Through alternated depositing porous SiO_2 nanoparticles (low refractive index) and dense TiO_2 layers on a TCO-coated glass substrate, Zhang et al.[101] first demonstrated color-tunable and opaque perovskite solar cells in 2015 (**Figure 11**c). These perovskite solar cells showed well-defined reflectance bands to produce varying colors, while the achieved efficiency was only 4%-9% in that time, which could be improved nowadays considering the great progress of perovskite solar cells in past years. A similar strategy has been successfully employed for a DSSC, in which TiO_2 also serves as the ETL material.[102] With the color-tunable mesoporous Bragg stack counter electrode, the resulted solid-state DSSC showed an PCE higher than that of the cell with conventional electrodes, as high as 7.1%. While the advantages and disadvantages of this method against the coating on glass have not yet been fully clarified in literature.

Besides using multilayered dielectric films, another nano-scaled optical structure, named optical cavity, has been proposed to be capable of well integrating with thin-film solar cells. According to a study from Lee et al.[103] in 2015, a colored a-Si solar cell was sandwiched by two metal layers (Ag), serving as both the electrode and the reflector (**Figure 11**d). Such a metal-semiconductor-metal structure, forming a Fabry-Pérot resonator, could selectively absorb partial light while reflecting the remaining to present different colors, by varying the thickness of the semiconductor layer. Nevertheless, its application in opaque solar cells will

inevitably lead to ultrathin photoactive layers and limited light absorption, resulting in the efficiency only around 3% when using an 18 nm a-Si photoactive layer.[103] To deal with this problem, Park et al.[104] proposed to exploit localized surface plasmon resonances by a single layer of subwavelength metallic nanowire arrays on a transparent substrate, which can achieve strong reflection in a specific wavelength range, with the spectral reflectance varying along with the thickness. By integrating these plasmonic color filters, vivid red, green and blue perovskite solar cells were demonstrated, providing a PCE of 10.12%, 8.17% and 7.72%, respectively.[104] Since the function of this method is similar to the Bragg reflector coating, a comparison between the two techniques in costs and compatibility may be the main concern.

4.3.2 Semitransparent Devices

Above-mentioned selective reflectors are generally placed on the top of absorbing materials, otherwise nearly all VIS light will be absorbed by the photoactive layer. But for semitransparent thin-film solar cells, whose photoactive layer is very thin or is segmented to only absorb partial light, adding a selective reflector at the back will be more meaningful, which can be designed to selectively reflect NIR and UV photons back to the photoactive layer, but only transmit specific VIS light. In this context, the poor performance of semitransparent thin-film solar cells due to the low photon-harvesting capacity can be improved, on the condition that a certain transmittance in VIS can still be kept, along with tunable color.

This idea was realized by Bronnbauer et al.[105] through integrating a printed dielectric mirror into the organic solar cell. Such a dielectric mirror, selectively reflecting NIR and transmitting VIS, could enhance the J_{sc} of a semitransparent polymer solar cell by up to 24%. These semitransparent devices can also present different colors using different layer configurations. It is remarkable that in this study the dielectric mirror was solution processed and printable,

enabling large-scale and low-cost production available.[105] To simultaneously reflect photons with wavelength below 400 nm and above 650 nm, Betancur et al.[106] designed a photonic multilayer, which is, otherwise, a non-periodic structure consisting of LiF and MoO_3. This method enhanced the PCE of a semitransparent PTB7:$PC_{71}BM$ organic solar cell by about 26%, along with the transparency in the VIS maintained at 30% and a PCE of 5.6%. Based on the photonic multilayer, the authors further demonstrated that color of the device can be broadly tuned with a very limited PCE variation (**Figure 11**e), opening a door for high-performance and colored semitransparent organic solar cells.

The optical cavity was also applied in colored and semitransparent a-Si solar cells,[107] with the back electrode in opaque devices[103] replaced by a transparent one. However, using the photoactive layer directly as the medium of the optical cavity is not an optimal design, since most light is either reflected or transmitted. Instead, this optical cavity should be better entirely placed at the back of photoactive materials, with a dielectric film as the medium. In this context, an optical cavity could serve as both an electrode and a color filter, to allow the light only in desired wavelength range transmit and reflect the other solar radiation back to photoactive materials to be reabsorbed. In other words, the non-wavelength-selective transparent electrode made by the ultrathin metal film is here replaced with a wavelength-selective electrode by inserting a dielectric film into the metal layer (**Figure 11**f).

Some practices can be found in both semitransparent organic[108, 109] and perovskite[110, 111] solar cells, and commonly Ag was adopted as the electrode, with the metal oxide materials like indium tin oxide (ITO), WO_3, TiO_2 as the dielectric film. For example, Shafian et al.[109] used solution-processed TiO2-AcAc as the dielectric component, which was sandwiched by two Ag layers in the anode. Results showed by varying thickness of the dielectric layer, ideal transmission spectra can be produced for different colors. Compared to a normal

semitransparent PTB7-Th: ITIC organic solar cell, PCE values of colored cells were around 5.6%, improved by over 55%. Due to the good wavelength-selective transmission and easy tunable color, this technique could stand as a good candidate for the cost-effective production of colored semitransparent solar cells in the future.

5. Challenges and Future Perspectives

Although the development of dedicated PVs for building integrations is not a major focus in the field of PV research and industry, great achievements have been made in the transparent and colored BIPV products for both commercialized and emerging PV technologies. After a systematically review on these achievements, here from a holistic perspective, some future directions in the following seven aspects are addressed for special concerns, which are supposed to be covered by extensive collaborations to accelerate the development of BIPV technologies.

5.1 Novel Design and Processing of Spatially Segmented TPVs

Although the spatially segmented TPV is not a new topic, recently the micro-structured design achieving visually stealth absorbing materials provides new chances in this field, but also poses significant challenges in the manufacture process. For solar PV panels based on well-established inorganic materials, it is required to develop a timesaving, low-cost and micron-accuracy processing method for the segmentation of absorbing materials, and its damage to the edge of absorbing materials should be minimized. Optimized pattern design is also of vital importance for achieving a trade-off between easy fabrication and attractive appearance. Rather than post-segmentation, the method of controlling material growth morphology to form a discontinues film can be more material-saving and economical, and whether these processing methods are amenable for mass production is still questionable. Besides, the possible short circuit due to the contact between cathodes and anodes in areas

without absorbing materials will reduce the J_{sc}, such issue has not yet been well clarified and addressed in literature.

5.2 Improving the Performance of Organic TPVs

The wavelength-selective organic/polymer solar cell holds the most promising candidate for TPVs with both high PCE and high AVT for now, which has been demonstrated by many proof-of-concept studies before, while further improvement is still required. Based on the theoretical analysis, the absorption onset of organic absorbers had better be further red-shifted, which desires for ultralow-bandgap organic semiconductors. Besides, there exists a huge current mismatch in the two-junction tandem solar cell based on a UV-harvesting perovskite and a NIR-harvesting NIR blend,[60] since the photocurrent generated by photons of UV light is much less than that by photons of NIR light. A multi-junction structure, such as a triple-junction tandem solar cell consisting of a high-bandgap perovskite, a middle-bandgap organic blend and a low-bandgap organic blend, may solve this issue. Moreover, optical optimization of the whole device should be paid more attention to further improve the EQE of TPV devices.

5.3 Stability and Scalability of Emerging PV Technologies

There are many advantages of emerging PV technologies in developing aesthetic BIPV products against traditional PV materials, especially for perovskite solar cells and organic solar cells. Despite enormous potential, the long-term stability and good scalability of these emerging technologies must be first achieved before competing with c-Si and those commercialized inorganic thin-film PV products. Addressing this issue requires combined efforts from both industry and research labs. Since the BIPV could be a good application candidate for these emerging PV technologies as means of entering the market, relevant studies of BIPV field should keep the latest achievements closely, ensuring that the stable and

high-performance BIPV products based on perovskite solar cells or organic solar cells can be realized as quickly as possible.

5.4 Photonic Management

Photonic management by a functional layer consisting of thin-film or nanoparticle materials plays a critical role in BIPVs, no matter for the transparency modification or color modification. Micro-nano optical materials and structures can be introduced to: (1) selectively reflect partial VIS light and transmit the remaining solar spectrum for opaque PVs with different colors; (2) selectively transmit partial VIS light and reflect the other solar spectrum for semitransparent PVs with different colors; (3) modify the spectral transmittance in the wavelength of VIS light to be uniform for wavelength-selective TPVs requiring a neutral color and a high CRI. To promote both aesthetic and high-performance BIPV products, more comprehensive studies on the applications of optical modification materials and structures in solar cells are urgently required, such as photonic crystals, optical cavities, plasmonic nanoparticles, metamaterials and surface textures, in order to achieve the desired absorption, reflection or transmission in the specific wavelength range.

5.5 Suppressing the Influence of Electrodes

Since BIPV devices should better keep a clear view for esthetic, the presence of electrodes may stand as great trouble. In colored PVs based on c-Si solar cells, the influence is relatively controllable when the color is produced on the layers above silicon solar cells, which could hide the under electrodes and cells. For both colored and transparent PVs based on those thin-film solar cells, highly transparent and conductive electrode materials are urgently needed. Especially for neutral-colored TPVs, in which transparent electrodes are required on both sides. Successfully demonstrated electrodes materials include transparent conductive oxides (TCOs) like ITO and FTO, ultrathin metals like Au and Ag, conductive polymers like

PEDOT: PSS, silver nanowire (Ag NW), carbon nanotube and graphene, with each one among them having limitations.[45, 112, 113] For example, the commonly used TCOs are bothered by the high-temperature and high-cost processing method, while the solution-processed Ag NWs suffer from a rough surface topology. Therefore, it is commonly recognized that developing electrodes with desired optical, electrical and processing properties are still full of challenges. Moreover, to simultaneously optimize the efficiency and esthetic, the combination of the photonic management with electrode materials is increasingly being recognized as an attractive topic.

5.6 Determining Cost-effective Color Modification Strategies

Although many strategies have been developed for the color modification of solar cells or modules, works on this topic are dispersed and unsystematic in the past. Comparing to TPV technologies, attention of research on colored PVs seems less focused, while the market of colored PVs could be more promising especially for those based on c-Si solar cells. Efforts should be paid on quantitatively clarifying the negative impact on the PCE of different methods, as well as their costs and abilities for large-scale manufacturing. A general color modification strategy, which will only introduce weak PCE reduction to solar cells but is low-cost to be achieved in production lines, would benefit the field. Additionally, cooperation between industry and scientific research will play a critical role in this stage, especially for those well-established PV technologies.

5.7 Standard Performance Evaluation

In addition to the indexes like PCE, J-V curve and EQE curve that are generally required for examining the performance of solar cells, aesthetic quality is also of critical importance to be accurately evaluated in the research of BIPVs. For neutral-colored TPVs, AVT, CRI and CIELAB color coordinates are essential, which should be tested and calculated based on the

spectral transmittance of a full device.[23] To avoid overestimation, independent measurements of *EQE(λ)*, *T(λ)*, and *R(λ)* are suggested, with the sum of these three values should not be greater than one. Besides, it is better to also provide the spectral transmittance of the pure photoactive layer for comparation, to clarify the influence of electrodes on AVT. While for colored opaque solar cells, the spectral reflectance and CIELAB color coordinates need to be provided and compared with that of the solar cell without color modification. Angle dependence of the color is also an important index. Moreover, BIPV usually refers to the installation on vertical facades, where the incident angle of solar radiation is relatively large, and the irradiation intensity will be usually reduced by the shadow, thus it is also encouraged to test the performance of a BIPV under conditions of large incident angle and low irradiation intensity. Moreover, a field test under outdoor real condition is suggested.

6. Outlook for Large-scale Implementations

To be implemented on a large scale rather than only in demonstration projects, BIPV products should not only be counted as power generation devices but more as building materials, arising many critical requirements (**Figure 12**). This review mainly deals with how the PV field can provide BIPV products meeting various aesthetic requirements of buildings worldwide. This is the first step that BIPVs can be widely accepted as building materials by the public since the aesthetic is the most intuitionistic factor, and also a factor only depending on the self-effort of the PV research and industry field.[114]

Costs and performance hold the body of BIPV technologies. Fast decreasing of PV costs is a central factor driving the rapid increasing rate of installation capacity, while prices of BIPVs have not yet fallen to the same extent. With investment increasing in BIPV markets and emerging of the above-mentioned advances, it is expected that the costs of BIPV products should essentially be not much higher than traditional PV products.[5] Because of the

compromise among transparency, color and efficiency, the PCE of BIPVs is inevitably lower than those general PV systems dedicated to power generation. Since differences in light intensity, irradiation angle, orientation and ambient temperature, the performance of different BIPV technologies may vary greatly which cannot be reflected by only the PCE tested under standard conditions. Hence, it is recommended that the yearly energy yield (kWh m^{-2}) in typical building application environment, which can be obtained by simulations or field tests, should be provided by the BIPV providers. Relevant test standards need be established.

Durability and safety issue are the foundations. Although commercialized PV systems have been confirmed to be durable through 25 years or even more over 30 years, the BIPV needs to further follow requirements in construction sectors, making the standardization of BIPV systems critical for guiding the development. Based on existing standards for both construction products and electrical components, general standardization and certification for BIPV materials, modules and systems are urgent to be established.[115]

In addition to these self-factors, extrinsic drivers and restraints also play critical roles in the development of BIPV markets to a large scale (**Figure 12**). Basic research in advanced BIPV technologies, which are addressed in this review, requires more efforts to promote the technology conversion from laboratories to industries. In the last decade, economic incentives have played significant roles in promoting the development of PV markets, and policies on advocating building energy saving are also driving the application of solar technologies in buildings. However, most countries have not yet identified specific incentives for BIPVs, which may be adverse for the BIPV market in the early stage when prices are relatively high.[116] Public awareness and extensive collaboration are more highlighted in BIPV markets against traditional PV markets since BIPV products are so close to people's daily lives while not widely recognized by the public. Effective communications among PV industries,

construction sectors and the public should be established, only on which condition that BIPV products addressing real needs can be quickly developed and spread.[117]

Sunlight is a fortune belonging to all people worldwide, no matter the race, region and economic level. Throughout history, solar energy utilization is always and has been a skill that is incorporated to our daily routine. Solar PVs, which emerge in the last several decades as the most concerned solar technology now, are expected to be very cheap, widespread, and common things all over the world. While aimless 'evolution' will ultimately lead to the most appropriate technology, the urgency of accelerating the energy transition necessitates a targeted progress of PV technologies, which is exactly the major prospect of this paper.

Acknowledgements

The authors would appreciate the financial support provided by the National Natural Science Foundation of China (NSFC) through Grant 51976124. Support from the RGC Research Impact Fund (Project No. RC2L) is also appreciated.

Conflict of Interest

The authors declare no conflict of interest.

References

[1] B. Energy, BP Energy Outlook: 2019 Edition, **2019**.
[2] IRENA, Global energy transformation: A roadmap to 2050 (2019 edition), **2019**.
[3] M. A. Alim, Z. Tao, M. K. Hassan, A. Rahman, B. Wang, C. Zhang, B. Samali, *Sol. Energy* **2019**, *188*, 1118.
[4] J. Yan, Y. Yang, P. Elia Campana, J. He, *Nat. Energy* **2019**, *4*, 709.
[5] C. Ballif, L.-E. Perret-Aebi, S. Lufkin, E. Rey, *Nat. Energy* **2018**, *3*, 438.
[6] W. Shockley, H. J. Queisser, *J. Appl. Phys.* **1961**, *32*, 510.
[7] A. Polman, M. Knight, E. C. Garnett, B. Ehrler, W. C. Sinke, *Science* **2016**, *352*, aad4424.
[8] P. K. Nayak, S. Mahesh, H. J. Snaith, D. Cahen, *Nat. Rev. Mater.* **2019**, *4*, 269.
[9] M. A. Green, E. D. Dunlop, J. Hohl-Ebinger, M. Yoshita, N. Kopidakis, A. W. Y. Ho-Baillie, *Progress in Photovoltaics: Research and Applications* **2020**, *28*, 3.
[10] T. N. Murakami, N. Koumura, *Adv. Energy Mater.* **2019**, *9*, 1802967.

[11] V. Rondán-Gómez, I. Montoya De Los Santos, D. Seuret-Jiménez, F. Ayala-Mató, A. Zamudio-Lara, T. Robles-Bonilla, M. Courel, *Applied Physics A* **2019**, *125*, 836.
[12] T. Gokmen, O. Gunawan, T. K. Todorov, D. B. Mitzi, *Appl. Phys. Lett.* **2013**, *103*, 103506.
[13] M. Liu, O. Voznyy, R. Sabatini, F. P. García de Arquer, R. Munir, Ahmed H. Balawi, X. Lan, F. Fan, G. Walters, Ahmad R. Kirmani, S. Hoogland, F. Laquai, A. Amassian, Edward H. Sargent, *Nat. Mater.* **2017**, *16*, 258.
[14] J. Yuan, A. Hazarika, Q. Zhao, X. Ling, T. Moot, W. Ma, J. M. Luther, *Joule* **2020**, *4*, 1160.
[15] M. Anaya, G. Lozano, M. E. Calvo, H. Míguez, *Joule* **2017**, *1*, 769.
[16] L. Shi, M. P. Bucknall, T. L. Young, M. Zhang, L. Hu, J. Bing, D. S. Lee, J. Kim, T. Wu, N. Takamure, D. R. McKenzie, S. Huang, M. A. Green, A. W. Y. Ho-Baillie, *Science* **2020**, *368*, eaba2412.
[17] N.-G. Park, K. Zhu, *Nat. Rev. Mater.* **2020**, *5*, 333.
[18] C.-Y. Liao, Y. Chen, C.-C. Lee, G. Wang, N.-W. Teng, C.-H. Lee, W.-L. Li, Y.-K. Chen, C.-H. Li, H.-L. Ho, P. H.-S. Tan, B. Wang, Y.-C. Huang, R. M. Young, M. R. Wasielewski, T. J. Marks, Y.-M. Chang, A. Facchetti, *Joule* **2020**, *4*, 189.
[19] J. Benduhn, K. Tvingstedt, F. Piersimoni, S. Ullbrich, Y. Fan, M. Tropiano, K. A. McGarry, O. Zeika, M. K. Riede, C. J. Douglas, S. Barlow, S. R. Marder, D. Neher, D. Spoltore, K. Vandewal, *Nat. Energy* **2017**, *2*, 17053.
[20] ISO, ISO 9050:2003, **2003**.
[21] ISO, ISO 10526:1999(E), **1999**.
[22] C. J. Traverse, R. Pandey, M. C. Barr, R. R. Lunt, *Nat. Energy* **2017**, *2*, 849.
[23] C. Yang, D. Liu, M. Bates, M. C. Barr, R. R. Lunt, *Joule* **2019**, *3*, 1803.
[24] R. R. Lunt, *Appl. Phys. Lett.* **2012**, *101*, 043902.
[25] L. Rakocevic, R. Gehlhaar, M. Jaysankar, W. Song, T. Aernouts, H. Fledderus, J. Poortmans, *J. Mater. Chem. C* **2018**, *6*, 3034.
[26] A. Takeoka, S. Kouzuma, H. Tanaka, H. Inoue, K. Murata, M. Morizane, N. Nakamura, H. Nishiwaki, M. Ohnishi, S. Nakano, Y. Kuwano, *Sol. Energy Mater. Sol. Cells* **1993**, *29*, 243.
[27] P. Fath, H. Nussbaumer, R. Burkhardt, *Sol. Energy Mater. Sol. Cells* **2002**, *74*, 127.
[28] E. Franklin, V. Everett, A. Blakers, K. Weber, *Adv. OptoElectron.* **2007**, *2007*.
[29] J. Yoon, A. J. Baca, S.-I. Park, P. Elvikis, J. B. Geddes, L. Li, R. H. Kim, J. Xiao, S. Wang, T.-H. Kim, M. J. Motala, B. Y. Ahn, E. B. Duoss, J. A. Lewis, R. G. Nuzzo, P. M. Ferreira, Y. Huang, A. Rockett, J. A. Rogers, *Nat. Mater.* **2008**, *7*, 907.
[30] C.-Y. Chen, T.-L. Chang, *Microelectron. Eng.* **2015**, *143*, 41.
[31] C.-Y. Tsai, C.-Y. Tsai, *Renewable Energy* **2020**, *145*, 2637.
[32] K. Lee, N. Kim, K. Kim, H.-D. Um, W. Jin, D. Choi, J. Park, K. J. Park, S. Lee, K. Seo, *Joule* **2020**, *4*, 235.
[33] S. Rahmany, L. Etgar, *ACS Energy Lett.* **2020**, *5*, 1519.
[34] S. Aharon, M. Layani, B.-E. Cohen, E. Shukrun, S. Magdassi, L. Etgar, *Adv. Mater. Interfaces* **2015**, *2*, 1500118.
[35] G. E. Eperon, V. M. Burlakov, A. Goriely, H. J. Snaith, *ACS Nano* **2014**, *8*, 591.
[36] G. E. Eperon, D. Bryant, J. Troughton, S. D. Stranks, M. B. Johnston, T. Watson, D. A. Worsley, H. J. Snaith, *The Journal of Physical Chemistry Letters* **2015**, *6*, 129.
[37] M. T. Hörantner, W. Zhang, M. Saliba, K. Wojciechowski, H. J. Snaith, *Energy Environ. Sci.* **2015**, *8*, 2041.
[38] L. Zhang, M. T. Hörantner, W. Zhang, Q. Yan, H. J. Snaith, *Sol. Energy Mater. Sol. Cells* **2017**, *160*, 193.
[39] R. Karsthof, P. Räcke, H. von Wenckstern, M. Grundmann, *Phys. Status Solidi A* **2016**, *213*, 30.

[40] A. J. Lopez-Garcia, A. Bauer, R. Fonoll Rubio, D. Payno, Z. Jehl Li-Kao, S. Kazim, D. Hariskos, V. Izquierdo-Roca, E. Saucedo, A. Pérez-Rodríguez, *Solar RRL* **2020**, *4*, 2000470.
[41] D. Liu, C. Yang, R. R. Lunt, *Joule* **2018**, *2*, 1827.
[42] E. Ravishankar, R. E. Booth, C. Saravitz, H. Sederoff, H. W. Ade, B. T. O'Connor, *Joule* **2020**, *4*, 490.
[43] S.-Y. Chang, P. Cheng, G. Li, Y. Yang, *Joule* **2018**, *2*, 1039.
[44] R. R. Lunt, V. Bulovic, *Appl. Phys. Lett.* **2011**, *98*, 113305.
[45] Q. Xue, R. Xia, C. J. Brabec, H.-L. Yip, *Energy Environ. Sci.* **2018**, *11*, 1688.
[46] C.-C. Chen, L. Dou, R. Zhu, C.-H. Chung, T.-B. Song, Y. B. Zheng, S. Hawks, G. Li, P. S. Weiss, Y. Yang, *ACS Nano* **2012**, *6*, 7185.
[47] K.-S. Chen, J.-F. Salinas, H.-L. Yip, L. Huo, J. Hou, A. K. Y. Jen, *Energy Environ. Sci.* **2012**, *5*, 9551.
[48] K. H. Hendriks, W. Li, M. M. Wienk, R. A. J. Janssen, *J. Am. Chem. Soc.* **2014**, *136*, 12130.
[49] Z. Liu, P. You, S. Liu, F. Yan, *ACS Nano* **2015**, *9*, 12026.
[50] Z. M. Beiley, M. G. Christoforo, P. Gratia, A. R. Bowring, P. Eberspacher, G. Y. Margulis, C. Cabanetos, P. M. Beaujuge, A. Salleo, M. D. McGehee, *Adv. Mater.* **2013**, *25*, 7020.
[51] C.-C. Chueh, S.-C. Chien, H.-L. Yip, J. F. Salinas, C.-Z. Li, K.-S. Chen, F.-C. Chen, W.-C. Chen, A. K. Y. Jen, *Adv. Energy Mater.* **2013**, *3*, 417.
[52] X. Hu, L. Chen, L. Tan, Y. Zhang, L. Hu, B. Xie, Y. Chen, *Sci. Rep.* **2015**, *5*, 12161.
[53] C.-Y. Chang, L. Zuo, H.-L. Yip, Y. Li, C.-Z. Li, C.-S. Hsu, Y.-J. Cheng, H. Chen, A. K. Y. Jen, *Adv. Funct. Mater.* **2013**, *23*, 5084.
[54] H. Yao, Y. Chen, Y. Qin, R. Yu, Y. Cui, B. Yang, S. Li, K. Zhang, J. Hou, *Adv. Mater.* **2016**, *28*, 8283.
[55] W. Wang, Q. Wu, R. Sun, J. Guo, Y. Wu, M. Shi, W. Yang, H. Li, J. Min, *Joule* **2020**, *4*, 1070.
[56] F. Liu, Z. Zhou, C. Zhang, J. Zhang, Q. Hu, T. Vergote, F. Liu, T. P. Russell, X. Zhu, *Adv. Mater.* **2017**, *29*, 1606574.
[57] W. Wang, C. Yan, T.-K. Lau, J. Wang, K. Liu, Y. Fan, X. Lu, X. Zhan, *Adv. Mater.* **2017**, *29*, 1701308.
[58] T. Li, S. Dai, Z. Ke, L. Yang, J. Wang, C. Yan, W. Ma, X. Zhan, *Adv. Mater.* **2018**, *30*, 1705969.
[59] H. Huang, X. Li, L. Zhong, B. Qiu, Y. Yang, Z.-G. Zhang, Z. Zhang, Y. Li, *J. Mater. Chem. A* **2018**, *6*, 4670.
[60] Q. Liu, L. G. Gerling, F. Bernal-Texca, J. Toudert, T. Li, X. Zhan, J. Martorell, *Adv. Energy Mater.* **2020**, *10*, 1904196.
[61] J. Zhang, G. Xu, F. Tao, G. Zeng, M. Zhang, Y. Yang, Y. Li, Y. Li, *Adv. Mater.* **2019**, *31*, 1807159.
[62] L. Zuo, X. Shi, W. Fu, A. K. Y. Jen, *Adv. Mater.* **2019**, *31*, 1901683.
[63] M. G. Debije, P. P. C. Verbunt, *Adv. Energy Mater.* **2012**, *2*, 12.
[64] X. Luo, T. Ding, X. Liu, Y. Liu, K. Wu, *Nano Lett.* **2019**, *19*, 338.
[65] Y. Zhao, R. R. Lunt, *Adv. Energy Mater.* **2013**, *3*, 1143.
[66] Y. Zhao, G. A. Meek, B. G. Levine, R. R. Lunt, *Adv. Opt. Mater.* **2014**, *2*, 606.
[67] C. Yang, M. Moemeni, M. Bates, W. Sheng, B. Borhan, R. R. Lunt, *Adv. Opt. Mater.* **2020**, *8*, 1901536.
[68] R. Rondão, A. R. Frias, S. F. H. Correia, L. Fu, V. de Zea Bermudez, P. S. André, R. A. S. Ferreira, L. D. Carlos, *ACS Appl. Mater. Interfaces* **2017**, *9*, 12540.
[69] C. Yang, W. Sheng, M. Moemeni, M. Bates, C. K. Herrera, B. Borhan, R. R. Lunt, *arXiv preprint arXiv:2009.09542* **2020**.

[70] F. Meinardi, F. Bruni, S. Brovelli, *Nat. Rev. Mater.* **2017**, *2*, 17072.
[71] W. Chen, J. Li, P. Liu, H. Liu, J. Xia, S. Li, D. Wang, D. Wu, W. Lu, X. W. Sun, K. Wang, *Solar RRL* **2017**, *1*, 1700041.
[72] F. Meinardi, H. McDaniel, F. Carulli, A. Colombo, K. A. Velizhanin, N. S. Makarov, R. Simonutti, V. I. Klimov, S. Brovelli, *Nat. Nanotechnol.* **2015**, *10*, 878.
[73] J. Roncali, *Adv. Energy Mater.* **2020**, *10*, 2001907.
[74] G. Wyszecki, W. S. Stiles, *Color science*, Vol. 8, Wiley New York, **1982**.
[75] Colour & Vision Research Laboratory (CVRL), http://cvrl.ioo.ucl.ac.uk/, Accessed: Jul. 14, 2020.
[76] A. Røyset, T. Kolås, B. P. Jelle, *Energy and Buildings* **2020**, *208*, 109623.
[77] J. Halme, P. Mäkinen, *Energy Environ. Sci.* **2019**, *12*, 1274.
[78] G. Peharz, A. Ulm, *Renewable Energy* **2018**, *129*, 299.
[79] J. Min, C. Bronnbauer, Z.-G. Zhang, C. Cui, Y. N. Luponosov, I. Ata, P. Schweizer, T. Przybilla, F. Guo, T. Ameri, K. Forberich, E. Spiecker, P. Bäuerle, S. A. Ponomarenko, Y. Li, C. J. Brabec, *Adv. Funct. Mater.* **2016**, *26*, 4543.
[80] M. Grätzel, *J. Photochem. Photobiol. C* **2003**, *4*, 145.
[81] Y. Cui, C. Yang, H. Yao, J. Zhu, Y. Wang, G. Jia, F. Gao, J. Hou, *Adv. Mater.* **2017**, *29*, 1703080.
[82] V. V. Brus, J. Lee, B. R. Luginbuhl, S.-J. Ko, G. C. Bazan, T.-Q. Nguyen, *Adv. Mater.* **2019**, *31*, 1900904.
[83] F. Frontini, P. Bonomo, E. Saretta, T. Weber, J. Berghold, in *32nd European Photovoltaic Solar Energy Conference and Exhibition*, 2016, 2498
[84] R. Schregle, M. Krehel, S. Wittkopf, *Buildings* **2017**, *7*, 72.
[85] S. Mertin, V. Hody-Le Caër, M. Joly, I. Mack, P. Oelhafen, J.-L. Scartezzini, A. Schüler, *Energy and Buildings* **2014**, *68*, 764.
[86] A. Soman, A. Antony, *Sol. Energy* **2019**, *181*, 1.
[87] N. Jolissaint, R. Hanbali, J.-C. Hadorn, A. Schüler, *Energy Procedia* **2017**, *122*, 175.
[88] J. Escarré, H. Li, L. Sansonnens, F. Galliano, G. Cattaneo, P. Heinstein, S. Nicolay, J. Bailat, S. Eberhard, C. Ballif, L. Perret-Aebi, "When PV modules are becoming real building elements: White solar module, a revolution for BIPV", presented at *2015 IEEE 42nd Photovoltaic Specialist Conference (PVSC)*, 14-19 June 2015, **2015**.
[89] Kromatix by SwissINSO, https://www.swissinso.com/, Accessed: 8 Jul., 2020.
[90] J. van Roosmalen, L. Slooff, L. Okel, T. Minderhoud, T. Sepers, A. Versluis, F. Frumau, M. Rietbergen, L. Polinder, E. Heller, *EUPVSEC, Amsterdam, 25-29 september 2017., 4 p.* **2017**.
[91] Kaleo Solar, http://www.kaleo-solar.ch/fr/index.php, Accessed: 8 Jul., 2020.
[92] D. Bouhafs, A. Moussi, A. Chikouche, J. M. Ruiz, *Sol. Energy Mater. Sol. Cells* **1998**, *52*, 79.
[93] I. Tobias, A. E. Moussaoni, A. Luque, *IEEE Trans. Electron Devices* **1999**, *46*, 1858.
[94] L. Zeng, M. Li, Y. Chen, H. Shen, *Sol. Energy* **2014**, *103*, 343.
[95] K. Ding, X. Zhang, L. Ning, Z. Shao, P. Xiao, A. Ho-Baillie, X. Zhang, J. Jie, *Nano Energy* **2018**, *46*, 257.
[96] J. H. Selj, T. T. Mongstad, R. Søndenå, E. S. Marstein, *Sol. Energy Mater. Sol. Cells* **2011**, *95*, 2576.
[97] G. Peharz, K. Berger, B. Kubicek, M. Aichinger, M. Grobbauer, J. Gratzer, W. Nemitz, B. Großschädl, C. Auer, C. Prietl, W. Waldhauser, G. C. Eder, *Renewable Energy* **2017**, *109*, 542.
[98] V. Neder, S. L. Luxembourg, A. Polman, *Appl. Phys. Lett.* **2017**, *111*, 073902.
[99] C.-Y. Tsai, C.-Y. Tsai, *Sol. Energy* **2018**, *170*, 419.
[100] G. Y. Yoo, J.-s. Jeong, S. Lee, Y. Lee, H. C. Yoon, V. B. Chu, G. S. Park, Y. J. Hwang, W. Kim, B. K. Min, Y. R. Do, *ACS Appl. Mater. Interfaces* **2017**, *9*, 14817.

[101] W. Zhang, M. Anaya, G. Lozano, M. E. Calvo, M. B. Johnston, H. Míguez, H. J. Snaith, *Nano Lett.* **2015**, *15*, 1698.
[102] C. S. Lee, J. T. Park, J. H. Kim, *J. Power Sources* **2016**, *324*, 637.
[103] K.-T. Lee, J. Y. Lee, S. Seo, L. J. Guo, *Light: Sci. Appl.* **2014**, *3*, e215.
[104] K.-T. Lee, J.-Y. Jang, J. Zhang, S.-M. Yang, S. Park, H. J. Park, *Sci. Rep.* **2017**, *7*, 10640.
[105] C. Bronnbauer, J. Hornich, N. Gasparini, F. Guo, B. Hartmeier, N. A. Luechinger, C. Pflaum, C. J. Brabec, K. Forberich, *Adv. Opt. Mater.* **2015**, *3*, 1424.
[106] R. Betancur, P. Romero-Gomez, A. Martinez-Otero, X. Elias, M. Maymó, J. Martorell, *Nat. Photonics* **2013**, *7*, 995.
[107] J. Y. Lee, K.-T. Lee, S. Seo, L. J. Guo, *Sci. Rep.* **2014**, *4*, 4192.
[108] Y. Kim, J. Son, S. Shafian, K. Kim, J. K. Hyun, *Adv. Opt. Mater.* **2018**, *6*, 1800051.
[109] S. Shafian, J. Son, Y. Kim, J. K. Hyun, K. Kim, *ACS Appl. Mater. Interfaces* **2019**, *11*, 18887.
[110] K.-T. Lee, M. Fukuda, S. Joglekar, L. J. Guo, *J. Mater. Chem. C* **2015**, *3*, 5377.
[111] J.-H. Lu, Y.-L. Yu, S.-R. Chuang, C.-H. Yeh, C.-P. Chen, *J. Phys. Chem. C* **2016**, *120*, 4233.
[112] Q. Tai, F. Yan, *Adv. Mater.* **2017**, *29*, 1700192.
[113] Z. Hu, J. Wang, X. Ma, J. Gao, C. Xu, K. Yang, Z. Wang, J. Zhang, F. Zhang, *Nano Energy* **2020**, *78*, 105376.
[114] S. L. Hille, H. C. Curtius, R. Wüstenhagen, *Energy and Buildings* **2018**, *162*, 21.
[115] K. A. Berger, S. Boddaert, M. D. Buono, Analysis of requirements, specifications and regulation of BIPV Analysis of requirements, specifications and regulation of BIPV, **2019**.
[116] H. C. Curtius, *Renewable Energy* **2018**, *126*, 783.
[117] F. J. W. Osseweijer, L. B. P. van den Hurk, E. J. H. M. Teunissen, W. G. J. H. M. van Sark, *Energy Procedia* **2017**, *111*, 974.
[118] T. S. Ustun, Y. Nakamura, J. Hashimoto, K. Otani, *Renewable Energy* **2019**, *136*, 159.
[119] L.-E. Perret-Aebi, P. Heinstein, V. Chapuis, C. Schlumpf, H.-Y. Li, C. Roecker, A. Schueler, V. Le Caër, M. Joly, R. Tween, Y. Leterrier, J.-A. Manson, J.-L. Scartezzini, C. Ballif, Vol. II, EPFL Solar Energy and Building Physics Laboratory (LESO-PB), 685.
[120] K. Yoshikawa, H. Kawasaki, W. Yoshida, T. Irie, K. Konishi, K. Nakano, T. Uto, D. Adachi, M. Kanematsu, H. Uzu, K. Yamamoto, *Nat. Energy* **2017**, *2*, 17032.
[121] E. H. Jung, N. J. Jeon, E. Y. Park, C. S. Moon, T. J. Shin, T.-Y. Yang, J. H. Noh, J. Seo, *Nature* **2019**, *567*, 511.
[122] M. Nakamura, K. Yamaguchi, Y. Kimoto, Y. Yasaki, T. Kato, H. Sugimoto, *IEEE J. Photovolt.* **2019**, *9*, 1863.
[123] T. Matsui, H. Sai, T. Suezaki, M. Matsumoto, K. Saito, I. Yoshida, M. Kondo, "Development of highly stable and efficient amorphous silicon based solar cells", presented at *Proc. 28th European Photovoltaic Solar Energy Conference*, **2013**.
[124] D. P. McMeekin, G. Sadoughi, W. Rehman, G. E. Eperon, M. Saliba, M. T. Hörantner, A. Haghighirad, N. Sakai, L. Korte, B. Rech, M. B. Johnston, L. M. Herz, H. J. Snaith, *Science* **2016**, *351*, 151.

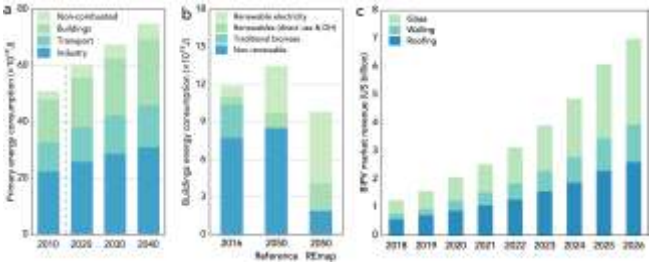

Figure 1. Pressure on energy saving and CO_2 emission reduction in building sector will drive the BIPV Market. a) Worldwide primary energy consumption by different end-use sectors. Data extracted from BP Energy Outlook.[1] b) Energy transformation pathways to 2050 in buildings promoted by IRENA. Data extracted from IRENA.[2] c) Worldwide BIPV commercial market revenue: 2018-2026, predicted by n-tech Research, 2017. Data extracted from Ballif et al.[5].

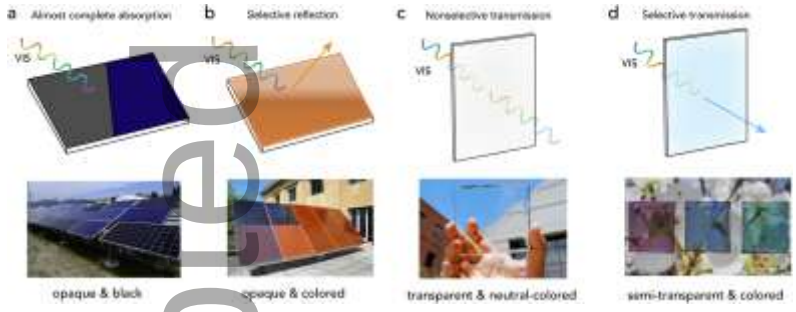

Figure 2. Schematic diagram of color and transparency of solar PVs. a) Diagram of routine PV modules that are opaque with black or dark-blue appearance. In these PV modules, visible light (VIS) is almost completely absorbed. b) Diagram of an opaque PV modules that are modified to display chromatic colors. Partial VIS must be selectively reflected to present color in these PV modules. c) Diagram of a transparent PV which is neutral-colored. VIS should be uniformly transmitted in part or whole to promise the neutral color. d) Diagram of colored and semitransparent PV. Various colors can be achieved by modifying diverse spectral transmittance in the wavelength of VIS. Photographs reproduced with permission from: a) Ustun et al.[118], Copyright 2019 Elsevier; b) Perret-Aebi et al.[119], Copyright 2014 CSEM; c) Traverse et al.[22], Copyright 2017 Springer Nature; d) Cui et al.[81], Copyright 2017 WILEY-VCH.

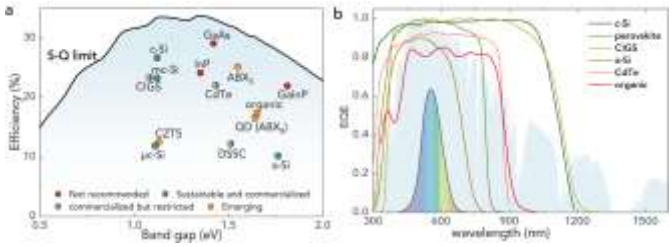

Figure 3. a) Shockley-Queisser detailed-balance efficiency limit (S-Q limit) and the present-day efficiency records of various solar cells. Solar cells are classified into 4 groups when considering their applications in BIPV, depending on whether they are commercialized and whether they have rare or toxic elements in semiconductor materials. The data of efficiency records extracted from Green et al.[9]. b) External quantum efficiency (EQE) curve of different types of solar cells with record efficiency, showing that the high-efficiency solar cells absorb almost all the visible light. The shadow behind the figure is the distribution of AM1.5 solar spectrum, and the chromatic region is the CIE 1924 photopic luminosity function defining the range of VIS. EQE data extracted from ref.[120] (c-Si), ref.[121] (perovskite), ref.[122] (CIGS), ref.[123] (a-Si), ref.[8] (CdTe), ref.[9] (organic).

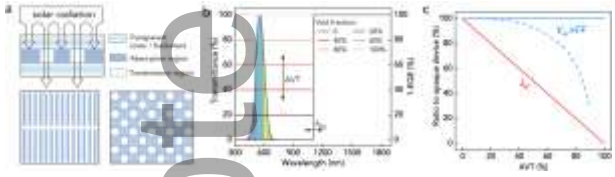

Figure 4. Schematic illustrations and theoretical analysis of spatially segmented TPVs. a) Schematic diagram presenting that the transparency is achieved by adding the space between opaque absorption materials, with the bottom figures showing two typical patterns. b) Transmittance as a function of wavelength, which equals to the void fraction in ideal cases when wavelength is smaller than the cut-off value λ_{Eg}. c) Schematic showing that in ideal cases, increasing AVT reduces short-circuit current J_{sc} proportionally, while having few impacts on the value of open-circuit voltage V_{oc} multiplying fill factor *FF* when AVT is not so big.

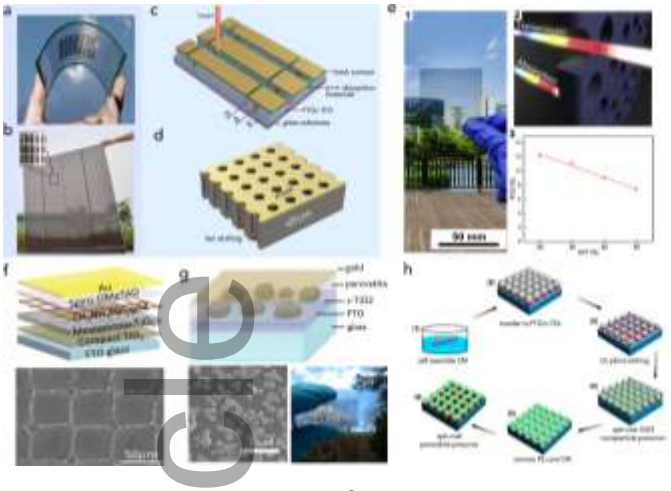

Figure 5. a-e) Examples of spatially segmented TPVs made by post-processing of absorption materials. a) A semitransparent c-Si submodule made by silicon strips. Reproduced under terms of the CC-BY license.[28] Copyright 2007 Evan Franklin et al. b) A semitransparent a-Si module made by laser scribing of a-Si films. Reproduced with permission.[31] Copyright 2020 Elsevier. Schematic of c) making semi-transparent thin-film solar cells by laser scribing and d) making semi-transparent silicon solar cells by chemical etching. e) A neutral-colored semi-transparent c-Si solar cell with its absorption materials undetectable: 1) photograph, 2) schematic showing light transmits through micro-holes, and 3) the PCE as a function of AVT. Reproduced with permission.[32] Copyright 2020 Elsevier.

f-h) Examples of spatially segmented PV cells made by controlling the solution-based fabrication process of perovskite thin films. f) A perovskite grid structure pattern formed by self-assembly: (top) device structure; (bottom) UHR-SEM image of the perovskite grid. Reproduced with permission.[34] Copyright 2015 WILEY- VCH. g) Perovskite islands fabricated by controlling the de-wetting process: (top) device structure; (bottom) SEM image of the perovskite islands and the photograph. Reproduced with permission.[35] Copyright 2013 American Chemical Society. h) The fabrication process of a patterned perovskite film based on SiO_2 honeycomb scaffold template. Reproduced with permission.[38] Copyright 2017 Elsevier.

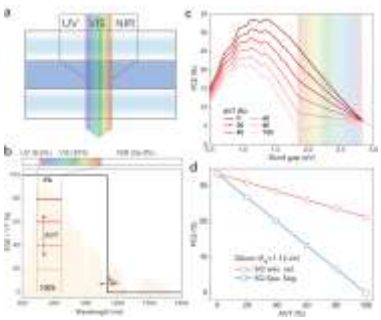

Figure 6. Working principles and theoretic analysis of wavelength-selective TPVs. a) Schematic showing a wavelength-selective TPV device selectively absorbs UV and NIR light while transmits VIS light. b) Ideal EQE curves of a wavelength-selective TPV device, showing that AVT increases by reducing EQE only in the wavelength of VIS. Ideally, the EQE plus transmittance (*T*) should equal to 1 as there is no reflection. c) PCE limit of single-junction TPVs, as a function of the bandgap, calculated based on the work of Lunt et al.[24]. d) Comparison of S-Q limit PCE in a wavelength-selective TPV and in a spatially segmented TPV, as a function of AVT, calculated using Si (E_g=1.12 eV) as an ideal absorber.

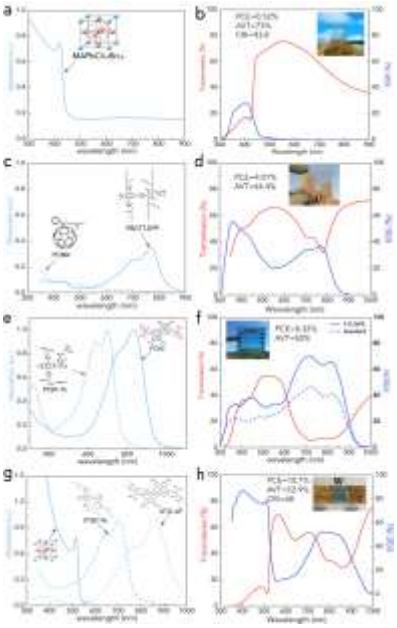

Figure 7. Wavelength-selective TPV devices with high AVT values. A UV-selective TPV based on a perovskite material with high bandgap: a) absorption spectra of $MAPbCl_{2.4}Br_{0.6}$ as the photoactive layer; b) the transmission, EQE and photograph of the TPV device. Adapted with permission.[41] Copyright 2018 Elsevier. An organic TPV using NIR-sensitive PBDTT-DPP as the donor and PCBM as the acceptor: c) absorption spectra of PBDTT-DPP and PCBM; d) the transmission, EQE and photograph. Adapted with permission.[46] Copyright 2012 American Chemical Society. An organic TPV using both a low-bandgap donor (PTB7-Th) and acceptor (FOIC): e) absorption spectra of PTB7-Th and FOIC; f) the transmission, EQE (the dotted line is the standard cell and the full line is the cell with a 1D nanophotonic structure) and photograph. Adapted with permission.[60] Copyright 2019 WILEY-VCH. A tandem TPV with both high AVT and efficiency, made by a ultralarge-bandgap perovskite as the top subcell and ultralow-bandgap organic materials as the bottom subcell: g) absorption spectra of $FAPbBr_{2.43}Cl_{0.57}$, PTB7-Th (donor) and 6TIC-4F (acceptor); h) transmission and EOE of the tandem device. Inserted photographs show (from left to right) a perovskite single-

junction, organic single-junction, and tandem TPV, respectively. Adapted with permission.[62] Copyright 2019 WILEY-VCH.

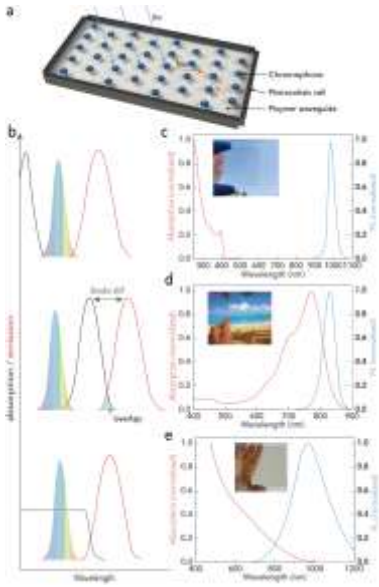

Figure 8. Neutral-colored transparent luminescent solar concentrators (LSC). a) Schematic showing the working principle and structure of LSCs, which are made of polymer waveguides incorporating chromophores and edge-mounted solar cells. b) Schematic diagram of absorption (black) and emission (red) spectra of chromophores which could be used for neutral-colored (semi-) transparent LSCs. From top to bottom: absorption in UV and re-emission in NIR, absorption in NIR and re-emission in deeper NIR, absorption in a larger spectral coverage and re-emission in NIR. c-e) Representative LSC devices, including photographs and the absorption and PL spectra of the incorporated chromophores. c) Adapted with permission.[64] Copyright 2018 American Chemical Society. d) Adapted with permission.[66] Copyright 2014 WILEY-VCH. e) Adapted with permission.[72] Copyright 2015 Springer Nature.

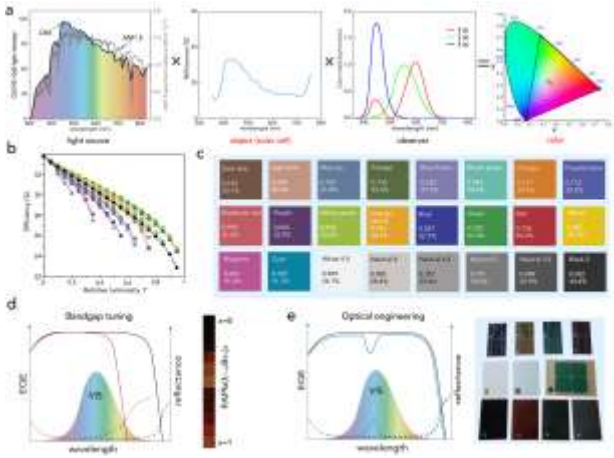

Figure 9. Design principles and methods for modifying PV colors. a) A Schematic showing factors determining the color of an object. From left to right: CIE1931 D65 light intensity and AM1.5 solar spectrum, spectral reflectivity of an object, CIE1931 color-matching functions representing the chromatic response of a standard observer, and CIE1931 color space chromaticity diagram. CIE standard data obtained from the database of CVRL.[75] b) Theoretical efficiency limits of different color as a function of relative luminosity, *Y*. Reproduced with permission.[77] Copyright 2019 The Royal Society of Chemistry. c) Theoretical efficiency limits of different colors, with the *Y* value of each color and corresponding efficiency limit presented. Reproduced with permission.[77] Copyright 2019 The Royal Society of Chemistry. d) Schematic showing that by bandgap tuning, the cut-off wavelength of absorbing materials in solar cells can shift into the wavelength range of VIS, resulting in different spectral reflectance and also a great influence on the EQE. The right photograph shows $FAPb[I_{(1-x)}Br_x]_3$ films with Br composition varying from x=0 to 1. Reproduced with permission.[124] Copyright 2016 Science (AAAS). e) Schematic showing that by optical engineering, solar PVs could selectively reflect part of VIS light to present colors, with EQE reduced only in that wavelength range. The right photograph shows some colored c-Si solar cells. Adapted with permission.[76] Copyright 2020 Elsevier.

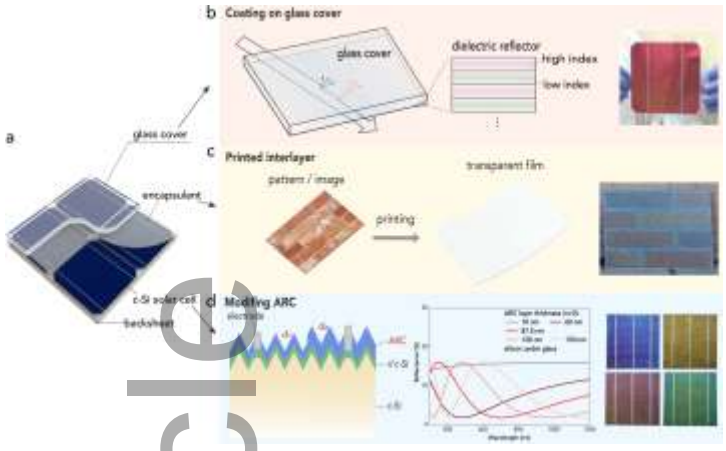

Figure 10. Practices of color modification on c-Si PV modules. a) The structure of a typical c-Si PV module. b) Schematic showing the inner side of the glass cover is coated with the Bragg Reflector which is made by alternating low and high refractive index dielectric materials, and a photograph of a c-Si solar cell under such a coated glass showing red color. c) Schematic showing modifying the appearance of PV module by adding an interlayer, which is made by printing specific patterns or images on a transparent film with semitransparent ink, and a photograph of a PV module with brick-like appearance. d) Schematic showing that c-Si solar cell can show various colors by modifying the anti-reflection coating (ARC). From left to right: structure of the front surface of c-Si solar cells, with ARC coating on the top; the simulated spectral reflectance of c-Si under glass, showing the influence of the thickness of single-layer ARC; and photographs of colored solar cells made by modifying the ARC. Inserted photographs are reproduced with permission: b) Soman et al.[86], Copyright 2019 Elsevier; c) Slooff et al.[90], Copyright 2017 EU PVSEC; d) Zeng et al.[94], Copyright 2014 Elsevier.

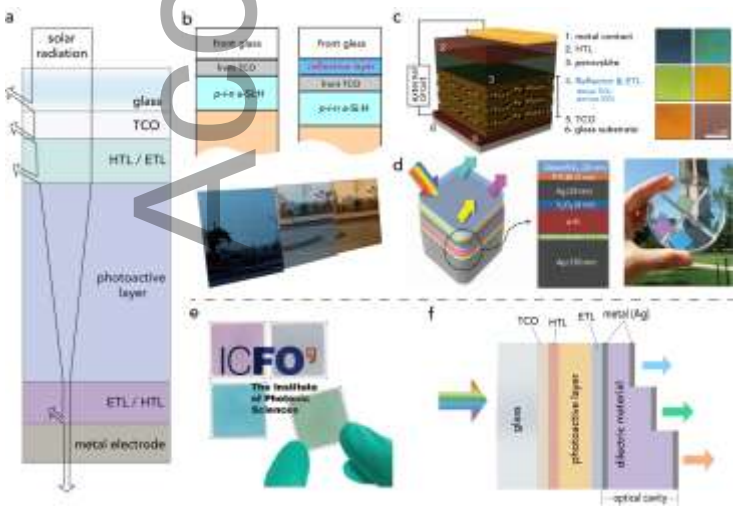

Figure 11. Practices of color modification on thin-film solar cells. a) Schematic illustration of light reflection, absorption and transmission in a thin-film solar cell. b) Structure of a regular

a-Si PV module and a colored module made by adding a wavelength-selective reflection layer on the glass, as well as photographs of colored a-Si BIPV modules. Reproduced with permission.[31] Copyright 2020 Elsevier. c) Perovskite solar cells with alternating layers of dense TiO_2 and porous SiO_2 forming a Bragg mirror to selectively reflect light: (left) device structure, (right) varying device colors by a different configuration of the Bragg mirror. Reproduced with permission.[101] Copyright 2015 American Chemical Society. d) Colored solar cells based on the a-Si absorber and a Fabry-Pérot (F-P) resonator formed by a metal-semiconductor-metal structure: (left) device structure, (right) photographs of colored devices. Reproduced with permission.[103] Copyright 2014 Springer Nature. e) Four semitransparent organic solar cells with different colors formed by using non-periodic photonic crystals, with colors tuned by varying the thickness of photonic crystal layers. Reprinted with permission.[106] Copyright 2013 Springer Nature. f) Schematic showing the structure of a thin-film solar cell integrated with the optical microcavity, which is composed of the dielectric layer sandwiched between the metal cathodes and could selectively transmit light by altering the thickness of the dielectric layer.

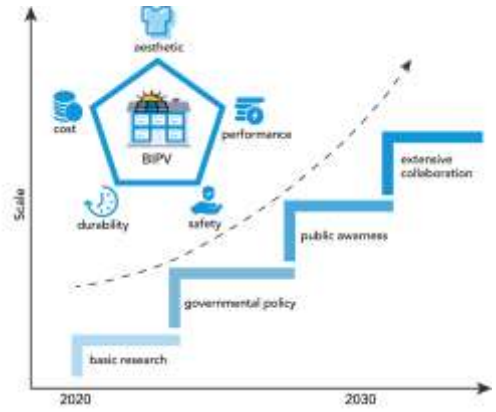

Figure 12. Schematic illustration of factors critical for the large-scale implementations of BIPV technologies. BIPV products must balance aesthetic, cost, performance, durability and safety for large-scale implementations. Besides, external conditions such as basic research, governmental policy, public awareness and extensive collaboration will play critical roles in the advance of BIPV technologies and their implementations.

Advances in solar photovoltaic technologies for the building integration are reviewed, with the focus on the transparent photovoltaic and the colored photovoltaic. Theoretical analysis, technical routes concerning materials and device structures, are highlighted for analyzing different methods. Finally, perspectives are presented to provide suggestions for further improving the performance of aesthetic building-integrated photovoltaics.

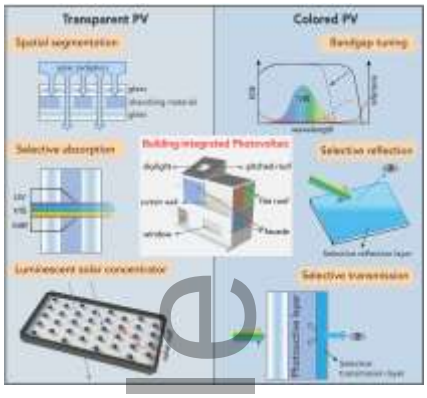

Zhenpeng Li received the B.E. degree from Shanghai Jiao Tong University (SJTU), China in 2019. He is now pursuing a Ph.D. degree with Dr. Tao Ma in the School of Mechanical Engineering, SJTU, China. Currently his research mainly focuses on solar energy utilization technologies, especially the interdisciplinary domain of micro-nano optics and solar photovoltaics.

Dr **Tao Ma** received his PhD from the Hong Kong Polytechnic University in 2015 and now he is an assistant professor at Shanghai Jiao Tong University. His research is mainly related to solar energy technologies and integrated photovoltaics. He has published over 60 peer-reviewed papers with an h-index of 24, including 10 ESI highly cited papers and 2 ESI hot papers. He received a number of awards during his early career stage, such as Excellent Young Scientist Award in 'Energy and Built Environment' and Outstanding PhD Thesis Award. He is also the editorial member of several journals including Applied Energy.

Prof. Hongxing Yang is now leading the Renewable Energy Research Group (RERG) at the Hong Kong Polytechnic University (PolyU). His research focuses on renewable energy applications and energy saving in buildings. Prof. Yang has completed over 60 projects and

obtained over HK$40 million grants. He has over 480 academic papers and 7 co-authored books published. He was on the list of 150 world most-cited researchers with impactful research in the disciplines of Civil Engineering, and he has been listed as “Highly Cited Researcher” from 2017 to 2020 reported from Clarivate. He is now serving Applied Energy as Editor and the Solar Energy Society of Hong Kong as President.

Ir Prof. **Lin Lu** is an outstanding researcher in building science and engineering with high local and international impact in both academia and industry. Prof. Lu joined the Hong Kong Polytechnic University as assistant professor in 2006, and was promoted to Professor in July 2018. She has published 5 books/handbook chapters and over 200 SCI-cited journal papers, resulting in an H-index of 42, and received the 2018 highly cited researcher by Clarivate Analytics in engineering. Her research findings have been adopted by researchers in over 60 countries and by the local government in its policy guidelines for renewable energy.

Prof. WANG Ruzhu (R. Z. Wang), distinguished chair professor, Shanghai Jiao Tong University. Director, Engineering Research Center of Solar Energy, MOE China. He has written 10 Books and about 500 co-authored international journal papers including EES, Joule and etc.. Due to his significant contributions in Sorption heat pumps, CCHPs, solar heating and cooling, and green building energy systems, Prof. Wang has received the J & E Hall International Gold Medal, the Nukiyama Memorial Award and the IIR-Gustav Lorentzen Medal. Prof. Wang is currently the Deputy editor-in-chief of Energy, Regional editor -International Journal of Refrigeration, associate editor of Solar Energy.